U.S. DEPARTMENT OF ENERGY | Office of Science

DOE/SC-ARM-16-002

Arctic Clouds Infrared Imaging Field Campaign Report

JA Shaw

March 2016

ARM CLIMATE RESEARCH FACILITY

DISCLAIMER

DOE/SC-ARM-16-002

Arctic Clouds Infrared Imaging Field Campaign Report

JA Shaw, Montana State University
Principal Investigator

March 2016

Work supported by the U.S. Department of Energy,
Office of Science, Office of Biological and Environmental Research

Executive Summary

The Infrared Cloud Imager (ICI), a passive thermal imaging system, was deployed at the North Slope of Alaska site in Barrow, Alaska, from July 2012 to July 2014 for measuring spatial-temporal cloud statistics. Thermal imaging of the sky from the ground provides high radiometric contrast during night and polar winter when visible sensors and downward-viewing thermal sensors experience low contrast. In addition to demonstrating successful operation in the Arctic for an extended period and providing data for Arctic cloud studies, a primary objective of this deployment was to validate novel instrument calibration algorithms that will allow more compact ICI instruments to be deployed without the added expense, weight, size, and operational difficulty of a large-aperture onboard blackbody calibration source. This objective was successfully completed with a comparison of the two-year data set calibrated with and without the onboard blackbody. The two different calibration methods produced daily-average cloud amount data sets with correlation coefficient = 0.99, mean difference = 0.0029 (i.e., 0.29% cloudiness), and a difference standard deviation = 0.054. Finally, the ICI instrument generally detected more thin clouds than reported by other ARM cloud products available as of late 2015.

Acronyms and Abbreviations

AON	Arctic Observing Network
ARM	Atmospheric Radiation Measurement Climate Research Facility
DOE	U.S. Department of Energy
ICI	Infrared Cloud Imager (instrument deployed during this IOP)
IOP	intensive operational period
NSA	North Slope of Alaska site
NSF	National Science Foundation
OD	Optical Depth

Contents

Figures

1.0 Background

This campaign resulted in a two-year deployment of Montana State University's third-generation Infrared Cloud Imager (ICI) instrument at the North Slope of Alaska (NSA) site near Barrow, Alaska, from 13 July 2012 to 22 July 2014. The primary purposes of the campaign were: 1) to collect continuous day-night measurements of Arctic cloud spatial distributions for at least one full year; and 2) to use these data to determine the accuracy with which long-term measurements can be calibrated with novel algorithms that adjust for the camera's changing response using internal data instead of real-time images of a large-area blackbody source. Logistical support was provided by the Atmospheric Radiation Measurement (ARM) Climate Research Facility of the U.S. Department of Energy (DOE) and primary financial support was provided by the National Science Foundation (NSF) Arctic Observing Network (AON) program (ARC 1108427, *Continuous spatial and radiative measurements of Arctic clouds leading to a network of compact infrared cloud imagers*). The Principal Investigator was Dr. Joseph Shaw from Montana State University in Bozeman, Montana, and the field engineer was Mr. Paul Nugent, also from Montana State University.

The ICI instrument was deployed close to the Great White facility at the North Slope of Alaska site and operated as autonomously as possible. The ICI instrument was operated 24 hours per day, 7 days per week, obtaining one cloud image at a user-selected interval that varied from approximately 1 minute and up. Typical operation was to obtain one image in a 1-5-minute period. During periods when more variability was expected, a high-temporal-resolution mode was employed, during which the imager acquired one image every few seconds. This mode was usually continued for several tens of minutes. The radiometrically calibrated thermal sky images were processed to remove atmospheric emission (using ARM-measured precipitable water vapor and air temperature). The resulting "residual radiance" images were used to identify cloud and no-cloud pixels in each image and to estimate the cloud optical depth for each cloudy pixel. These image sequences were processed to produce histograms of cloud fraction by season and month. A particularly noteworthy product of this campaign was separate cloud histograms for daytime and nighttime, focusing on the ICI's unique ability (relative to a visible imager) to obtain measurements with unchanging sensitivity during day and night.

The ICI technique relies on the naturally high radiometric contrast that exists between the down-welling thermal emission from a cloud and the clear sky (Shaw and Nugent 2013; Shaw et al. 2005). Whereas a downward-viewing sensor frequently has difficulty identifying clouds because of low radiometric contrast with the surface, an upward-viewing sensor sees the cloud against a very cold, weakly radiating atmosphere. This contrast is particularly high in the dry Arctic atmosphere because the primary source of long-wave IR clear-sky emission is water vapor.

At the heart of the ICI instrument deployed in this campaign is a small thermal infrared camera for which radiometric calibration was achieved with two different methods: 1) using real-time images of a large-area blackbody source; and 2) using advanced algorithms that track the changing camera response and monitor the changing camera offset using an internal shutter as an equivalent external blackbody (Nugent et al. 2013a; Nugent et al. 2014). The instrument was packaged in a weatherproof housing and connected via Ethernet connection to a control computer and the Internet. The optics module was located outside and the computer was inside a nearby shelter to provide remote instrument control and data acquisition. Figure 1 shows the ICI-3 in Barrow during the 2012-2014 deployment. The IR camera viewed the sky through an open hole that was covered by a hatch between image acquisitions and during precipitation.

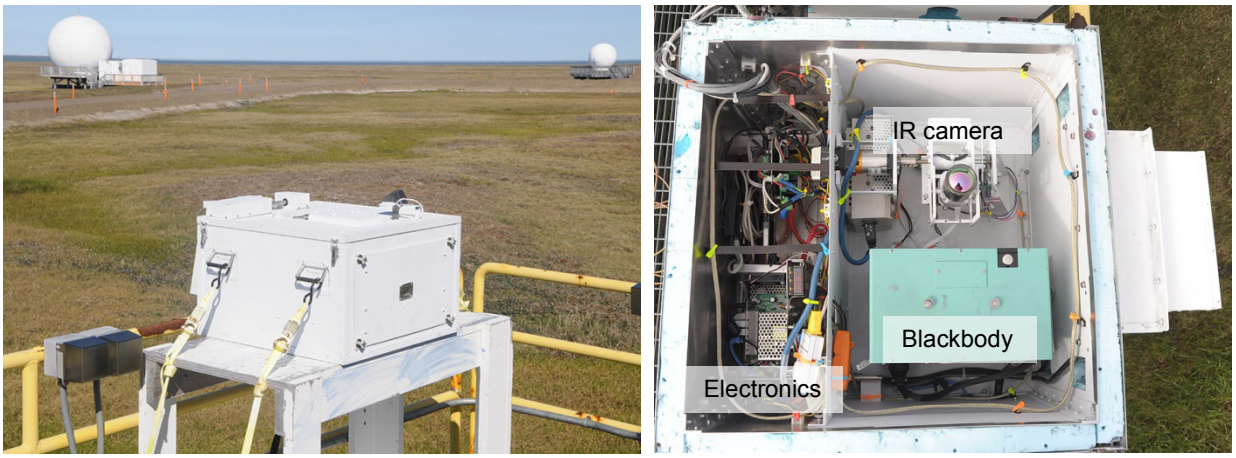

Figure 1. The ICI exterior (left) and interior (right) in Barrow, Alaska, during the 2012-2014 deployment. The right-hand photo shows the IR camera looking up (upper right), large-area blackbody calibration source (green box, lower right), and electronics, left.

The infrared camera in the ICI system images the down-welling radiance in a wavelength band of approximately 8-13.5 μm, a "window region" of high atmospheric transmittance in the absence of clouds. Nevertheless, reliable cloud detection measurements require careful removal of the clear-sky emission. This is done in the earlier ICI algorithms with a curve-fit relation developed from radiative transfer models, using precipitable water vapor and air temperature as inputs (Shaw et al. 2005; Thurairajah and Shaw 2005). The wider-angle ICI systems also incorporate measured pixel angles to account for off-zenith angular variation of the atmospheric emission (Nugent et al. 2009a; Nugent et al. 2013b; Shaw and Nugent 2013).

Raw digital images from the thermal camera were calibrated to produce radiance images [W/(m^2 sr)]. An independent calibration was used for each pixel to achieve high image uniformity and accuracy. The camera has an uncooled microbolometer detector array (Kruse 2001), removing the need for liquid nitrogen or mechanical cryo-coolers. We have expended great effort to develop and validate techniques for calibrating these room-temperature detectors at the low levels of Arctic atmospheric emission (Shaw et al. 2005; Nugent et al. 2009a, b; Nugent et al. 2013a, 2014).

ICI radiance images contain emission from the atmosphere and from clouds, if present. Clouds are identified by removing the clear-sky atmospheric emission component and comparing the residual radiance to a threshold determined from the calibration and atmospheric models based on historic radiosonde data. Thin ice clouds are the most difficult to detect, but experiments with the ICI, a cloud lidar, and radiosondes have shown that even sub visual cirrus clouds can be detected with care, visible cirrus clouds with OD > 0.25 are identified readily, and thicker clouds are detected easily. Our more advanced algorithms use temporal variations of pixel brightness and angular gradients of measured radiance to obtain better thin-cloud sensitivity than could be achieved with radiometric thresholding alone because the largest radiometric uncertainty arises typically from the clear-sky atmospheric emission model, not the camera calibration.

2.0 Notable Events or Highlights

In accordance with AON Program policy, the focus of our efforts has been on collecting and validating the Arctic cloud data rather than conducting intensive data analysis. However, several examples are included here to demonstrate the value of the data obtained in the campaign. Figure 2 shows a radiance image (left), processed to produce a conventional binary cloud map showing clear and cloudy pixels (center), and a cloud map showing the visible cloud optical depth estimated for each pixel (right). The ability of the ICI instrument to map the variability in cloud optical depth provides much greater information for studies of cloud spatial radiative properties. Note also that the bright spot in the upper-right corner of the radiance image, corresponding to the dark region in the cloud mask and cloud OD image, marks the location of the sun. The ICI systems require no sun occulter and we simply track the sun's location and remove the affected pixels during processing.

Figure 2. ICI images from Barrow: radiance in W m-2 sr-1 (left), conventional binary cloud map showing cloudy and clear pixels (center), and cloud map showing upper-limit cloud optical depth (right).

The value of the optical depth retrieval capability is illustrated further in Figure 3, which shows a time-series plot of ICI total cloud amount (black line), ICI "thin cloud amount" (OD < 2, green line), and "thick cloud amount" (OD > 2, red line). Although the black line indicates that this day had nearly constant 100% cloud cover, the ICI cloud classification data show that the sky was covered with thin clouds early, and thick clouds later. The down-welling long-wave radiative forcing measured by the ICI (residual radiance multiplied by the field of view solid angle) increased from +5 W/m^2 in the morning to more than +20 W/m^2 in the afternoon.

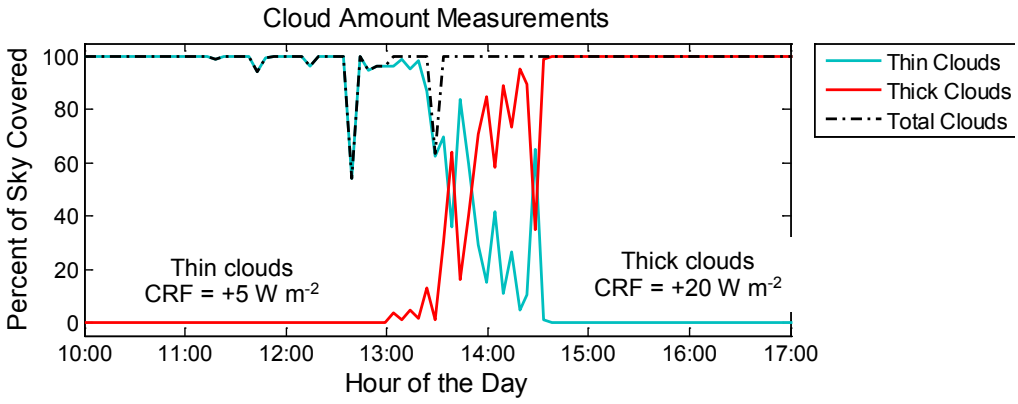

Figure 3. ICI cloud amount plotted versus time for total, thin-cloud amount, and thick-cloud amount. The down-welling long-wave cloud radiative forcing (CRF) increased from +5 to more than +20 W/m^2 with essentially no change in the total cloud amount because of changing cloud optical depth.

3.0 Lessons Learned

There were many lessons learned, but one of the primary ones to note for the future was that the instrument operated especially well after we found an all-metal replacement for a critical gearbox mounted on the motor that pointed the small infrared camera alternately at the blackbody calibration source and the sky port. Despite an impressive cold-weather rating, the original gearbox turned out to contain plastic gears that eventually broke in the cold.

4.0 Results

Following calibration, quality-control checks, and removal of atmospheric emission, the ICI data were processed to generate a time series of cloud amount (% of pixels containing clouds), which were averaged by day and month. Figure 4 shows a two-year time-series plot of daily cloud amount for the complete deployment from July 2012 to July 2014, indicating that the instrument operated nearly continuously except for a few long gaps for maintenance in summer and early fall, 2013. Figure 5 shows a climatology of monthly-average cloud amount that uses blue and yellow colors to separately indicate thin and thick clouds, respectively. In this case, "thin" means clouds with visible optical depth less than 2 and "thick" means clouds with optical depth greater than 2. The data set used to create this figure was processed to includes all clouds with estimated OD ≥ 0.25, below which special processing is required to consistently avoid false detections. These results show an annual-averaged total cloud amount of 0.84, higher than the combined radar-lidar estimate of 0.78 and ceilometer estimate of 0.75 found for Barrow data from 1998 to 2008 (Dong et al. 2010), but nearly identical to the results reported by Shupe et al. (2011) for Barrow and with a very similar annual cycle as found in both of these previous studies.

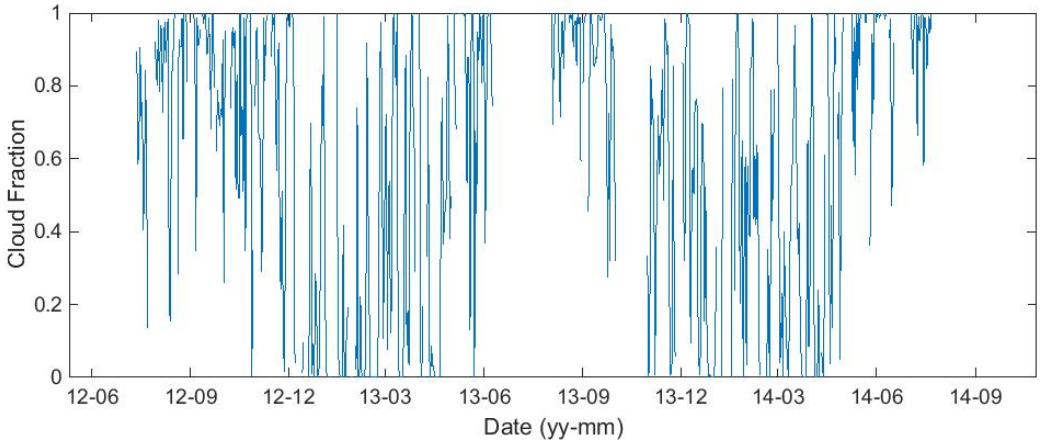

Figure 4. Daily average cloud amount for the complete two-year deployment from July 2012 to July 2014 (dates on the horizontal axis are labeled according to yy-mm).

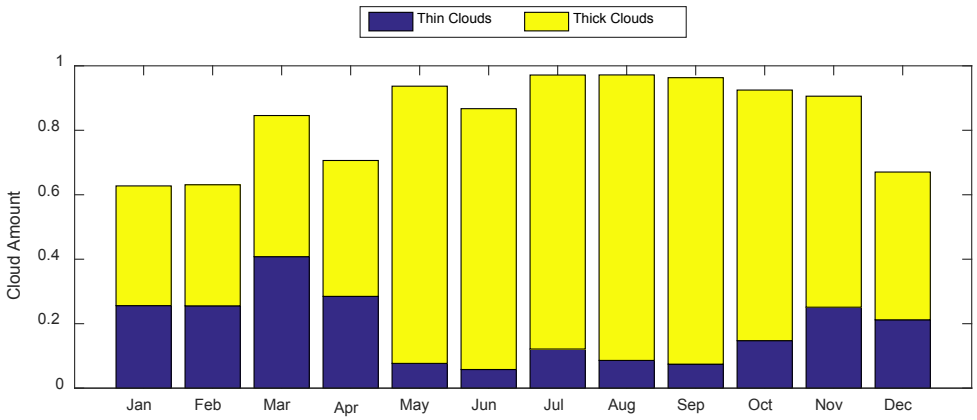

Figure 5. Monthly averaged cloud amount measured by the ICI at Barrow, Alaska during 2012-2014 ("thick clouds" are OD ≥ 2 and "thin clouds" are OD < 2).

One of the interesting results of this deployment was that the ICI data reported a significant number of thin clouds that were not detected or not counted as clouds by the other ARM sensors. Unfortunately, during this deployment the upgraded cloud radar and high-spectral-resolution lidar both generated data that were still marked as "suspect" as of the writing of this report, and the micropulse lidar was reporting spurious clouds that we do not yet understand, so we had limited cloud data to compare with. However, we did compare our measurements with those from the ceilometer (CEIL) on 530 days of common operation, the Total Sky Imager or TSI (visible-wavelength all-sky imager) for the 346 common operating days, and the Skyrad and MFRSR estimates of cloud fraction for the 202 and 124 days, respectively, with common data. The most meaningful of these comparisons is with ICI and CEIL, which is summarized in the daily average cloud amount scatterplots in Figure 6. These plots are for the ICI data calibrated with the onboard blackbody. The left-hand plot is for ICI data with estimated cloud OD ≥ 1.0 (correlation coefficient = 0.90, mean difference = -0.066, standard deviation = 0.16), while the right-hand plot is for ICI data with cloud OD ≥ 0.25 (correlation = 0.81, mean difference = 0.036, standard deviation = 0.21). Given the frequent spatial heterogeneity of thin clouds, it is not surprising that the zenith-pointing ceilometer and most-of-sky-viewing ICI disagree mostly for thin clouds. However, this difference also could result partly from thin ice clouds near the ground. It is important to note that for this comparison with the ceilometer and for other comparisons with the other ARM cloud sensors, the correlation coefficient was highest when the ICI data with OD < 0.25 were neglected, meaning that the ICI instrument frequently detected thin clouds that were either not detected or not classified as clouds by the other sensors.

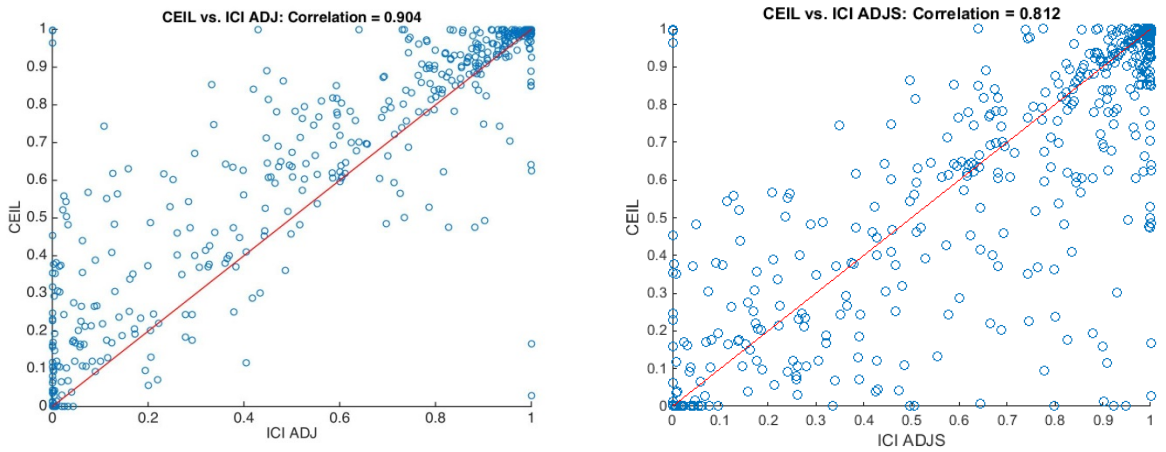

Figure 6. Scatterplots of daily average cloud fraction measured by the ceilometer (vertical) and the ICI calibrated with the onboard blackbody (horizontal axis). The left plot only includes ICI data with cloud OD ≥ 1.0, while the right plot includes ICI data with OD ≥ 0.25.

Note that there are ICI images in which even lower-OD clouds are apparently present, but the 0.25 value is the threshold above which the routine processing algorithms have proven reliable. It would be useful to conduct future deployments that include careful human observations of diamond dust and ice fog as ground truth to carefully document the ICI thin cloud sensitivity at Barrow in winter.

One of the most important results of this study is the comparison of ICI results with and without the use of an onboard blackbody calibration source. Figure 7 shows the results of this comparison as a scatterplot of daily cloud amount derived from the two calibration methods. The vertical axis shows data calibrated with the onboard blackbody and the horizontal axis shows data calibrated without the blackbody (instead relying on our advanced algorithms that track the changing camera response using internal camera measurements [Nugent et al. 2013a; 2014]). This figure indicates that the adaptive algorithms performed extremely well, producing data that agreed with the blackbody-calibrated data with a correlation coefficient of 0.990, a mean difference of 0.0029 (i.e., a difference of 0.29% cloud fraction), and a difference standard deviation of 0.054. This is an extremely encouraging result, which indicates that future ICI instruments can be made with notably lower cost, smaller size, and lower weight. In fact, our analysis shows that the differences in this figure are smaller than or comparable to the uncertainties in the blackbody source accuracy over the wide-angle field of view.

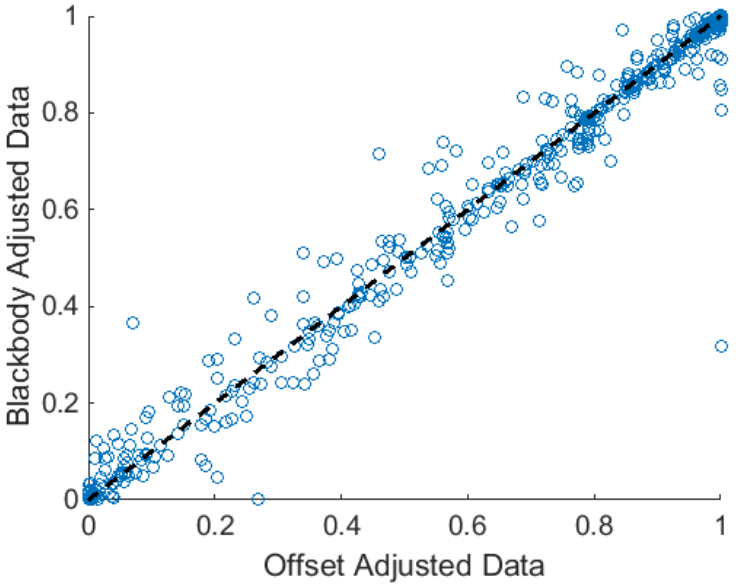

Figure 7. Scatterplot of ICI data calibrated with the onboard blackbody (vertical) and with the adaptive calibration algorithms (horizontal) after removal of a constant offset that arose from the pre-deployment laboratory calibration (correlation = 0.990, mean difference 0.0029, standard deviation = 0.054).

5.0 Arctic Clouds Infrared Imaging Publications

In accordance with AON Program policy, our main efforts have been on collecting and validating Arctic cloud data. Therefore, the publications related to this campaign focus on instrument calibration methods, the ICI method in general, and the use of the ICI camera calibration algorithms in related atmospheric imaging applications.

5.1 Journal Articles/Manuscripts

Vollmer, M, JA Shaw, and PW Nugent. "Visible and invisible mirages: Comparing inferior mirages in the visible and thermal infrared." *Applied Optics* 54(4): B76-B84 (2015), doi:10.1364/AO.54.000B76.

Shaw, JA, PW Nugent, and M Vollmer. 2015. "Infrared moon imaging for remote sensing of atmospheric smoke layers." *Applied Optics* 54(4): B64-B75, doi:10.1364/AO.54.000B64.

Nugent, PW, JA Shaw, and NJ Pust. 2014. "Radiometric calibration of infrared imagers using an internal shutter as an equivalent external blackbody." *Optical Engineering* 53(12): 123106, doi:10.1117/1.OE.53.12.123106.

Nugent PW, and JA Shaw. 2014, "Calibration of uncooled LWIR microbolometer imagers to enable long-term field deployment." *Proceedings of SPIE* 9071 (*Infrared Imaging Systems: Design, Analysis, Modeling, and Testing XXV*, G. C. Holst, K. A. Krapels, G. H. Ballard, J. A. Buford, and R. L. Murrer, eds.), 90710V, doi:10.1117/12.2053082.

Shaw, JA, and PW Nugent. 2013. "Physics principles in thermal infrared imaging of clouds in the atmosphere." *European Journal of Physics* 34(6): S111-S121, doi:10.1088/0143-0807/34/6/S111.

Nugent, PW, JA Shaw, and S Piazzolla. 2013. "Infrared cloud imager development for atmospheric optical communication characterization, and measurements at the JPL Table Mountain Facility," Interplanetary Network Progress Report 42-192, 1-30, http://ipnpr.jpl.nasa.gov/progress_report/42-192/192C.pdf.

Nugent, PW, JA Shaw, and NJ Pust. 2013. "Correcting for focal plane array temperature dependence in microbolometer infrared cameras lacking thermal stabilization." *Optical Engineering* 52(6): 061304, doi:10.1117/1.OE.52.6.061304.

Shaw, JA, PW Nugent, NJ Pust, BJ Redman, and S Piazzolla, 2012. "Cloud optical depth measured with ground-based, uncooled infrared imagers," *Proceedings of SPIE* 8523 (*Remote Sensing of the Atmosphere, Clouds, and Precipitation IV*), 85231D, Kyoto, Japan.

5.2 Meeting Abstracts/Presentations/Posters

Vollmer, M, JA Shaw, and PW Nugent. "Visible and invisible mirages: comparing inferior mirages in the visible and thermal infrared spectral range," *11th International Meeting on Light and Color in Nature*, University of Alaska, Fairbanks, AK (5-8 August 2013).

Vollmer, M, K.-P Möllmann, JA Shaw, and PW Nugent. "Messungen der temperature des Mondes mit thermokameras vom Erdboden," invited paper, Temperatur conference, Berlin, Germany (5-6 June 2013).

Shaw, JA, PW Nugent, and M Roddewig. "Infrared Cloud Imager cloud measurements at Barrow, Alaska," Proceedings of the Atmospheric System Research Conference, (http://asr.science.energy.gov/meetings /stm/posters/poster_pdf/2013/P001002.pdf), Potomac, Maryland (18-21 March 2013).

Reynolds, A, PW Nugent, and JA Shaw. "Producing and testing infrared cloud imaging systems," Student Research Celebration, Montana State University, Bozeman, MT, 15 Apr. 2014.

Lommatsch, G, PW Nugent, and JA Shaw. "Infrared cloud imager data analysis for optical satellite communication," Student Research Celebration, Montana State University, Bozeman, MT, 15 Apr. 2014.

Holmes, W, PW Nugent, and JA Shaw. "Micro wind turbine power for infrared cloud imager instrumentation," Student Research Celebration, Montana State University, Bozeman, MT, 15 Apr. 2014.

Redman, B, PW Nugent, and JA Shaw. "Validation of a low-cost all-sky infrared cloud imager," Student Research Celebration, Montana State University, Bozeman, MT, 15 Apr. 2014.

Redman, B, PW Nugent, S Piazzolla, and JA Shaw. "Testing a low-cost all-sky infrared cloud imager," Optical Technology Center (OpTeC) Annual Meeting, Montana State University, Bozeman, MT, 15 Aug. 2013.

Roddewig, M, PW Nugent, JA Shaw. "Infrared cloud imager measurements at Barrow, Alaska," Optical Technology Center (OpTeC) Annual Meeting, Montana State University, Bozeman, MT, 15 Aug. 2013.

Redman, B, PW Nugent, S Piazzolla, and JA Shaw. "Testing a low-cost all-sky infrared cloud imager," Student Research Celebration, Montana State University, Bozeman, MT, 18 April 2013.

Roddewig, M, PW Nugent, JA Shaw. "Infrared cloud imager measurements at Barrow, Alaska," Student Research Celebration, Montana State University, Bozeman, MT, 18 April 2013.

Shaw, JA, PW Nugent, J Johnson. "Radiometric infrared imaging with compact microbolometer cameras: from clouds to beehives," invited talk at *Infrared: science, technology, and applications,* 506th Wilhelm and Else Heraeus-Seminar, Bad Honnef, Germany, 21-23 May 2012.

6.0 References

Kruse, PW. 2001. *Uncooled Thermal Imaging: Arrays, Systems, and Applications*, SPIE Press (Bellingham, WA) TT51 (90 pp).

Nugent, PW, JA Shaw, and S Piazzolla. 2009a. "Infrared cloud imaging in support of Earth-space optical communication." *Optics Express* 17(10): 7862-7872, doi:10.1364/OE.17.007862.

Nugent, PW, JA Shaw, NJ Pust, and S Piazzolla. 2009b. "Correcting calibrated infrared sky imagery for the effect of an infrared window." *Journal of Atmospheric and Oceanic Technology* 26(11): 2403-2412, doi:10.1175/2009JTECHA1288.1.

Nugent, PW, JA Shaw, and NJ Pust. 2013a. "Correcting for focal-plane-array temperature dependence in microbolometer infrared cameras lacking thermal stabilization." *Optical Engineering* 52(6): 061304, doi:10.1117/1.OE.52.6.061304.

Nugent, PW, JA Shaw, and S Piazzolla, 2013b. "Infrared cloud imager development for atmospheric optical communication, characterization, and measurements at the JPL Table Mountain Facility." *Interplanetary Network Progress Report* 42-192, 1-30, http://ipnpr.jpl.nasa.gov/progress_report/42-192/192C.pdf.

Nugent, PW, JA Shaw, and NJ Pust. 2014. "Radiometric calibration of infrared imagers using an internal shutter as an equivalent external blackbody." *Optical Engineering* 53(12): 123106, doi:10.1117/1.OE.53.12.123106.

Nugent, PW, and JA Shaw. 2014. "Calibration of uncooled LWIR microbolometer imagers to enable long-term field deployment." *Proc. SPIE* 9071, 90710V.

Shaw, JA, PW Nugent, NJ Pust, B Thurairajah, and K Mizutani. 2005. "Radiometric cloud imaging with an uncooled microbolometer thermal infrared camera." *Optical Express* 13(15): 5807-5807. http://www.opticsexpress.org/abstract.cfm?id=85237

Shaw, JA, PW Nugent, NJ Pust, BJ Redman, and S Piazzolla. 2012. "Cloud optical depth measured with ground-based, uncooled infrared imagers." *Proc. SPIE* 8523, 85231D.

Shaw, JA and PW Nugent. 2013. "Physics principles in thermal infrared imaging of clouds in the atmosphere." *European Journal of Physics* 34(6): S111-S121.

Shupe, MD, VP Walden, E Eloranta, T Uttal, JR Campbell, SM Starkweather, and M Shiobara. 2011. "Clouds at Arctic atmospheric observatories. Part I: Occurrence and macrophysical properties." *Journal of Applied Meteorology and Climatology* 50: 626–644, doi:10.1175/2010JAMC2467.1.

Thurairajah, B, and JA Shaw, 2005. "Cloud statistics measured with the Infrared Cloud Imager (ICI)." *IEEE Transactions on Geoscience and Remote Sensing* 43(9): 2000–2007. http://ieeexplore.ieee.org/stamp/stamp.jsp?arnumber=1499016

www.arm.gov

U.S. DEPARTMENT OF
ENERGY

Office of Science